NAG 5-814
IN-46-CR
325892
P.39

# GPS Measurements of Strain Accumulation Across the Imperial Valley, California: 1986-1989

**Shawn Larsen**
Seismological Laboratory
California Institute of Technology; Pasadena, CA 91125

**Robert Reilinger**
Earth Resources Laboratory
Massachusetts Institute of Technology; Cambridge, MA 02139

## Abstract

GPS data collected in southern California from 1986 to 1989 indicate considerable strain accumulation across the Imperial Valley. Displacements are computed at 29 stations in and near the valley from 1986 to 1988, and at 11 sites from 1988 to 1989. The earlier measurements indicate 5.9 ± 1.0 cm/yr right-lateral differential velocity across the valley, although the data are heavily influenced by the 1987 Superstition Hills earthquake sequence. Some measurements, especially the east-trending displacements, are suspect for large errors. The 1988-1989 GPS displacements are best modeled by 5.2 ± 0.9 cm/yr of valley crossing deformation, but rates calculated from conventional geodetic measurements (3.4 - 4.3 cm/yr) fit the data nearly as well. There is evidence from GPS and VLBI observations that the present slip rate along the southern San Andreas fault is smaller than the long-term geologic estimate, suggesting a lower earthquake potential than is currently assumed. Correspondingly, a higher earthquake potential is indicated for the San Jacinto fault. The Imperial Valley GPS sites form part of a 183 station network in southern California and northern Baja California, which spans a cross-section of the North American-Pacific plate boundary. Once data from this network are fully analyzed, the strain distribution across the San Andreas, San Jacinto, and Elsinore faults will be well established.

(NASA-CR-187788) GPS MEASUREMENTS OF STRAIN ACCUMULATION ACROSS THE IMPERIAL VALLEY, CALIFORNIA: 1986-1989 (California Inst. of Tech.) 39 p CSCL 08G
N91-15649
Unclas
H1/46 0325892

## 1. Introduction

The Global Positioning System (GPS) is rapidly becoming one of the most important tools to study tectonic deformation. Signals from earth-orbiting NAVSTAR satellites (NAVigation Satellite Time And Ranging) are inverted to obtain 3-dimensional coordinates of geodetic monuments with high precision. For crustal deformation studies, the relative position (or baseline) between stations is often measured. Under optimal conditions, the typical accuracy for a 50 km baseline is about 1 cm in the horizontal and 3 cm in the vertical [e.g., *Davis et al.*, 1989]. The accuracy is significantly degraded from poor observing conditions. GPS measurements can be used to monitor the secular deformation associated with plate motion, or to record the rapid strain fluctuations due to seismic and volcanic activity. GPS technology is ideally suited for crustal motion research since, unlike conventional geodesy, intersite visibility is not required, stations can be separated by long distances (> 100 km), and it is possible to measure 3-dimensional deformation.

A prime location for GPS studies is the Imperial Valley of southern-most California (Figure 1). The valley is one of the most tectonically active regions in the state and has been the site of several large earthquakes. In fact, GPS monitoring was initiated in 1986 with resurveys in 1988 and 1989. GPS station displacements from 1986 to 1988 have been discussed by *Larsen et al.* [1991a]. These measurements illustrate the effect of the 1987 Superstition Hills earthquake sequence. In the present study we incorporate the 1989 GPS observations. Significant station displacements are observed across the Imperial Valley between 1986 and 1989. These movements are attributed in part to the relative motion between the North American and Pacific plates.

## 2. Seismicity and Tectonics

The Imperial Valley (Figure 1) is a complex transition zone between crustal spreading in the Gulf of California and right-lateral transform motion along the San Andreas fault [*Lomnitz et al.*, 1970; *Elders et al.*, 1972]. The valley is 4 - 12 million years old and is filled by up to 15 km of late Cenozoic sediments [*Larson et al.*, 1968; *Moore and Buffington*, 1968; *Ingle*, 1974; *Fuis et al.*, 1982]. The structural axis of the valley and its major fault systems trend to the northwest, roughly parallel to the Pacific-North American plate motion. A significant fraction of the relative plate displacement may be accommodated across the valley.

The Imperial Valley is one of the most seismically active regions of California with much of the activity occurring along the Imperial fault and in the Brawley Seismic Zone [*Johnson and Hill*, 1982]. Several large earthquakes have occurred in and near the Imperial Valley since 1940. The Imperial fault ruptured with a $M_S$ 7.1 event in 1940 and a $M_L$ 6.6 event in 1979 [*U. S. G. S.*, 1982]. Segments of the San Jacinto fault system broke with a $M_L$ 6.2 earthquake in 1954 and a $M_L$ 6.5 event in 1968 (Borrego Mountain). The most GPS relevant episode of seismic activity occurred recently along the Superstition Hills segment of the San Jacinto fault system [e.g., *Magistrale et al.*, 1989]. On November 24, 1987, a large ($M_S$ 6.2) earthquake occurred along a northeast-trending seismic lineament; 12 hours later a larger event ($M_S$ 6.6) occurred along the northwest-trending Superstition Hills fault. What makes this earthquake sequence so significant from a GPS standpoint, is that it occurred within a preexisting GPS network.

Conventional geodetic measurements indicate significant displacement across the Imperial Valley, which is inferred to represent interplate deformation. Triangulation data averaged between 1941 and 1986 suggest 4.3 cm/yr right-lateral movement oriented N40°W across the valley [*Snay and Drew*, 1988]. The observed deformation is time dependent, with rates of 6.1, 2.1, and 4.5 cm/yr for the intervals 1941-1954, 1954-1967, and 1967-1979, respectively. The high velocity for the earliest period supports the hypothesis of northwestward strain migration following the 1940 earthquake [*Thatcher*, 1979; *Reilinger,* 1984]. Furthermore, the computed station displacements indicate that north of the Imperial fault interplate deformation is distributed over a zone at least 50 km wide, whereas to the south interplate deformation is concentrated within a 20 km wide zone centered along the Imperial fault. Trilateration measurements made by the U.S. Geological Survey from 1972 to 1987 indicate 3.45 cm/yr right-lateral displacement between stations on opposite sides of the Imperial Valley [*Prescott et al.*, 1987a; *Prescott et al.*, 1987b]. These differential movements are oriented approximately N40°W. No significant change in station velocities are observed following the 1979 Imperial Valley earthquake [*Savage et al.*, 1986].

New global plate models (NUVEL-1) predict the Pacific-North American relative velocity averaged over the last several million years to be 4.7 cm/yr oriented N39.6°W at Imperial Valley coordinates (115.5°W, 33.0°N) [*DeMets et al.*, 1987; *DeMets et al.*, 1990]. VLBI observations during the 1980's suggest a similar present-day rate [e.g., *Clark et al.*, 1987; *Kroger et al.*, 1987]. The conventional geodetic data in the Imperial Valley indicate a significant fraction of this motion may be distributed along faults in this region.

### 3. GPS Observations

The data presented here were obtained in a series of GPS field campaigns in 1986, 1988, and 1989. In all, a total of 32 Imperial Valley stations have been occupied more than once between 1986 and 1989. Here we discuss data collection and processing methods used for each survey. The 1986 and 1988 campaigns are described in more detail by *Larsen* [1991].

The National Geodetic Survey (NGS) began GPS observations in southern California with a 54 station network in 1986; 42 stations were located in or near the Imperial Valley (Figure 2). TI-4100 GPS receivers were used for all data collection. Each of the

20 days of observation were processed independently utilizing the GPS22 software developed at the NGS, with satellite orbit parameters provided by the NSWC (Naval Surface Weapons Center). Station coordinates were obtained from the daily intersite GPS vectors by utilizing the geodetic adjustment program DYNAP (DYNamic Adjustment Program) [*Drew and Snay*, 1989]. This was one of the first GPS networks established to investigate crustal motion. GPS surveying at this time was still at an "experimental stage." The data collection methods used during 1986 were not suitable for obtaining the highest accuracy solutions. In addition, due to a variety of equipment and logistical problems, a significant amount of data were lost. Because of these unfortunate circumstances, the quality of the data was fairly poor. The positional uncertainties for the 1986 survey are suggested to be approximately 1 ppm (parts per million). This is equivalent to a 5 cm error for a 50 km baseline.

During late February and early March, 1988, university GPS crews (UNAVCO) occupied 19 sites in the Imperial Valley, including 15 marks observed in 1986 (Figure 2). The NGS returned to the Imperial Valley the following month and reoccupied 21 of the previously established monuments. TI-4100 receivers were used for all measurements. Data from both surveys were processed independently with the Bernese GPS software package from the University of Bern in Switzerland. For each campaign, the data were combined into one multiday solution. The Cartesian coordinate differences from the university and NGS surveys were adjusted by least squares to obtain station positions for 1988. Satellite orbits were improved with the aid of fiducial observations from Mojave (California), Westford (Massachusetts), and Richmond (Florida), made as part of the Cooperative International GPS Network (CIGNET) [*Chin*, 1987]. The horizontal precision for intersite vectors when orbit improvement techniques are used is about 0.03 ppm [e.g., *Davis et al.*, 1989; *Dong and Bock*, 1989]. This is equivalent to sub-centimeter level uncertainty for line-lengths less than a few hundred kilometers.

During March, 1989, university groups occupied 28 geodetic marks in the vicinity of the Imperial Valley, 19 of which were previously surveyed in 1986 or 1988 (Figure 3). Several new marks were established north of the Salton Sea in the Coachella Valley. While most data were collected with TI-4100 GPS instruments, this campaign differed from previous surveys in that Trimble-4000SD receivers were used at some sites. The field experiment was conducted at a time of anomalously high solar flare activity which created large ionospheric disturbances [*Jackson et al.*, 1989]. The ionosphere creates a frequency dependent delay for the GPS multi-signal structure, composed of two carrier phase transmissions at 1575.42 MHz (L1) and 1227.60 MHz (L2) [e.g., *King et al.*, 1985]. For dual frequency observations (L1 and L2), the ionospheric contribution (error) is removed by an appropriate combination of the two phase observables. However, if only single frequency measurements are available (either intentionally or due to poor observing conditions), the positioning accuracy of all but the shortest baselines will be seriously degraded. The 1989 phase observations contained a disproportionate number of cycle slips and data gaps, presumably due to the poor ionospheric conditions. The TI-4100 instruments generally collected both the L1 and L2 phase signals, so the ionospheric effect could be eliminated. The Trimble 4000SD receivers, however, experienced significant difficulty maintaining phase-lock on the L2 frequency (it is found that newer Trimble models, specifically the 4000SST, are not as susceptible to solar activity). In fact, between 30 - 60 percent of the L2 data (Trimble 4000SD) were lost. It is unlikely that the centimeter level accuracy required for this study could be achieved solely with the L1 frequency. Therefore, data collected with Trimble 4000SD instruments were not used, although we are currently working on schemes to utilize these measurements through ionospheric modeling constrained by the dual frequency TI-4100 data. Continental fiducial phase observations from the CIGNET tracking sites were either nonexistent or of extremely poor quality, presumably due to the poor ionospheric conditions. Therefore, we were unable to apply orbit improvement techniques. A multiday solution was obtained with the Bernese software utilizing the broadcast orbits. Positioning errors with the broadcast ephemerides are believed to be 0.1 - 1.0 ppm.

## 4. GPS Displacements

GPS displacement vectors for the intervals 1986-1988 and 1988-1989 are shown in Figures 4 and 5, respectively. All measurements are made relative to station OCTI. Formal estimates of GPS uncertainty almost always underestimate variances derived from repeatability studies. We define more realistic errors by multiplying the formal covariance matrix calculated with the GPS solution by an estimated variance factor, which scales as the average baseline length. For the 1986-1988 displacements, we assume a variance factor so that the average baseline error is 5 cm, or 1 ppm for a 50 km line. The large uncertainty is due to the quality of the 1986 data. For the 1988-1989 displacements, the average baseline error is assumed 2 cm, or 0.4 ppm for a 50 km line. The largest component of uncertainty is attributed to the broadcast orbits used for the 1989 solution. In a similar sized network spanning the Santa Barbara channel, *Larsen et al.* [1991b] found 1 - 3 cm discrepancies between line-lengths obtained with the broadcast ephemeris and those obtained by utilizing orbit improvement techniques. Our approach for handling uncertainties, albeit somewhat ad hoc, allows for self consistent relative errors and it illustrates the much larger uncertainties in the east-trending direction ($\sim 4$ times larger than the north-trending errors). This effect is due to the predominantly north-south ground track of the satellite orbits, which significantly improves positional accuracy along this orientation.

Displacements for the 1986-1988 interval (Figure 4) are complicated by the 1987 Superstition Hills earthquake sequence, as well as large measurement uncertainties. The seismic effects are clearly demonstrated in the GPS vectors; displacements at KANE and L589 approach 0.5 meters. Estimates of fault rupture indicate 10 stations near the seismic rupture zone moved at least 5 cm [*Larsen et al.*, 1991a]. The displacements are consistent with 109 cm right-lateral slip along the Superstition Hills fault and 45 cm left-lateral slip along the Elmore Ranch fault. Still, there is a considerable component of southeast-trending movement which can not be explained as seismic deformation or measurement uncertainty. This is evident when the displacements are decomposed into their north and east-trending components (Figures 6). Decomposing vector displacements into geographic components tends to separate the uncertainties, which are magnified in the longitudinal direction. Each component is plotted as the distance from OCTI on a cross section trending N50°E, perpendicular to the North American-Pacific relative plate motion (N40°W). Simple dislocation theory [e.g., *Mansinha and Smylie*, 1971] is used to remove the effect of the 1987 Superstition Hills earthquake sequence from the observed displacement field, following fault models suggested by *Larsen* [1991]. Therefore, Figure 6 represents the nonseismic deformation across the Imperial Valley.

The north-trending 1988-1989 movements clearly exhibit right-lateral displacement; stations to the northeast are offset to the south relative to sites on the other side of the valley. Stations displaying the largest scatter are for the most part, those sites where the applied seismic correction is greater than 4 cm (Figure 6, open circles). This suggests fault-rupture complexities not accounted for by the uniform dislocation model used to remove the effects of the 1987 earthquake [*Larsen*, 1991]. The east-trending movements exhibit large scatter with no discernible trend across the valley. This is invariant of the size of the seismic displacement, so the scatter can not be explained simply as unmodeled seismic effects. Presumably, the large deviations are due to the fairly significant east-trending errors in the 1986 data. This may explain the anomalous vector displacements observed in Figure 4, especially noticeable for those sites near the border east of the Imperial fault.

The nonseismic north-trending GPS displacements indicate an 8.1 $\pm$ 1.3 cm offset across the Imperial Valley (Figure 6). This differential movement is calculated by linearly fitting those data furthest to the southwest and northeast. The data errors are increased by 0.33 times the estimated seismic displacements, giving less weight to those stations most affected by the 1987 earthquakes. The east-trending components are not used due to the large data scatter. The 8.1 cm offset is assumed to represent plate-boundary deformation. If we assume a uniform velocity field parallel to the direction of plate motion (N40°W), the observed north-trending offset is equivalent to 5.9 ± 1.0 cm/yr right-lateral movement across the GPS network.

The 1988-1989 station displacements clearly demonstrate right-lateral southeast-trending movement across the Imperial (Figure 5). Stations furthest to the northeast are displaced approximately 5 cm to the southeast relative to sites on the other side of the valley. The observed motion at some sites (e.g., BLAC) may be attributed to the larger east-trending uncertainties. These measurements demonstrate how easily GPS can monitor tectonic deformation, even over time scales as short as 1 year. The 1988-1989 displacements are also decomposed into their north and east-trending components (Figure 7). Right-lateral differential movement across the GPS network is indicated in both components.

The north-trending offset observed between 1988 and 1989 (Figure 7) is smaller than that from 1986 to 1988 (Figure 6) because of the shorter observation period (1.0 years). However, the more recent measurements are not influenced by seismic activity and contain smaller experimental error. Since the 1988-1989 GPS station coverage is more uniformly distributed across the valley, it is difficult to constrain an absolute differential offset. Instead, the measurements are modeled assuming a semi-infinite right-lateral shear plane at depth representing the Pacific-North American plate margin (Figure 8). The plane is oriented N40°W about coordinates 32.796°N, 115.454°W, almost congruent with the Imperial fault and the axis of the Salton Trough. The upper depth is constrained at 10 km and uniform slip is assumed over the entire shear boundary. *Snay and Drew* [1988] incorporate a similar model to explain triangulation observations between 1941 and 1986, but allow additional slip along the Imperial fault necessitated by their detailed station coverage in this region. More complex models assuming distributed offset along the Imperial, San Andreas, San Jacinto, and Elsinore faults, and within the Brawley Seismic Zone, have been used to model additional geodetic measurements in the valley [e.g., *Savage et al.*, 1979]. The measurements presented here are not of sufficient resolution or accuracy (due to the short time coverage) to warrant such detail. The 1988-1989 GPS displacement vectors are best constrained by 5.2 ± 0.9 cm/yr plate-boundary deformation. The best-fit solution to the observed GPS movements is shown in Figure 7. Additional solutions are obtained by varying the depth to the upper boundary of the shear plane from 5 to 15 km. The calculated displacement rates range from 4.4 (5 km) to 6.0 cm/yr (15 km). The minimum residual solution is obtained at 10 km depth (5.2 cm/yr).

## 5. Discussion

### Deformation across valley

The 1986-1988 measurements are concentrated along the Imperial fault (Figure 4). The nonseismic displacements reveal a sharp 15 - 20 km wide boundary between deformation on either side of the Imperial Valley (Figure 6). This suggests that strain is accommodated exclusively along the Imperial fault in the southern half of the valley. The 1988-1989 measurements are distributed more uniformly throughout the region (Figure 5), and indicate a broader strain-transition zone (Figure 7). This implies that deformation may be occurring along several structures to the north, including the San Andreas, San Jacinto, and Elsinore faults. The same pattern is observed in the conventional geodetic measurements, which indicate concentrated strain in a narrow 20 km wide zone about the Imperial fault, and diffuse deformation of at least 50 km wide to the north [*Snay and Drew*, 1988; *Prescott et al.*, 1987b].

The GPS obtained rates of deformation across the Imperial Valley, as well as those derived through conventional geodetic techniques, are listed in Table 1. These are compared with the estimated velocity between the Pacific and North American plates (NUVEL-1), and rates derived from VLBI measurements between stations along the western coast of California and within the stable North American continent. Because the 1988-1989 GPS displacements are not affected by seismic deformation, we speculate that this interval yields a more reliable estimate of strain across the Imperial Valley than the 1986-1988 measurements. The 1988-1989 GPS deformation rate is comparable to the relative plate velocity. This suggests that all plate motion is concentrated across the valley, with little or no deformation west of the Elsinore fault. However, the conventional measurements taken over the last 50 years indicate significantly smaller rates, thus requiring additional slip on faults not spanned by the networks to satisfy the plate velocity.

GPS and trilateration (EDM) provide comparable accuracies, and both are considerably more precise than triangulation. However, the EDM observations span a 15 year period, while only 3 years of GPS coverage are available. Therefore, the trilateration rate should more accurately reflect the deformation in this region, which suggests the GPS measurements over-estimate the true displacement. In fact, a 3.4 cm/yr deformation rate fits the 1988-1989 GPS observations nearly as well (Figure 7). An alternate explanation is accelerated deformation between 1986 and 1989. The triangulation data indicate time-dependent displacements. Between 1941 and 1954 the calculated rate is significantly greater than the average between 1941 and 1986, although this is attributed to post-seismic effects following the 1940 Imperial Valley earthquake. No increased rate is observed following the 1979 earthquake [*Savage et al.*, 1986]. There is marginal evidence for a regional strain fluctuation (increase) during 1978 and 1979 throughout southern California, but the nature of this apparent deformation is uncertain [*Savage et al.*, 1981; *Savage et al.*, 1986]. Given the large uncertainties for the GPS estimates (~ 1 cm), it is not possible with the available data to distinguish if there has been increased deformation over the last several years.

### Earthquake potential: Imperial and southern San Andreas faults

The earthquake recurrence interval along the Imperial fault is estimated using the geodetically determined strain rates. The 1940 Imperial Valley earthquake ruptured the entire length of the Imperial fault. Approximately 3.0 and 4.5 m slip (coseismic plus postseismic) are estimated for the northern and southern segments of the fault, respectively [*Reilinger*, 1984]. Surface offsets were as great as 6 m south of the border with displacements tapering off rapidly to the north [*Trifunac and Brune*, 1970; *Sharp*, 1982]. Surface rupture was confined to the fault north of the border during the 1979 earthquake. Geodetic and strong ground motion modeling suggest an average slip of about 1 m along the 1979 rupture plane, with patches of higher displacement (asperities) [e.g., *Hartzell and Heaton*, 1983; *Archuleta*, 1984; *Reilinger and Larsen*, 1986].

At an observed strain rate of 4 - 5 cm/yr and per-event-ruptures between 1 and 3 m, a 20 - 75 year earthquake recurrence interval is calculated for the northern Imperial fault. This assumes all strain is released during major seismic episodes. This recurrence rate is comparable to the 32 year earthquake repeat time suggested by *Sykes and Nishenko* [1984] and the ~ 50 year interval predicted by *Anderson and Bodin* [1987].

The relative velocities of 3 Imperial Valley GPS sites are well constrained from VLBI observations since 1979 [*Clark et al.*, 1987; *Sauber et al.*, 1989; *Ma et al.*, 1989]. The GPS and VLBI computed deformation rates between BLAC and PINY and between BLAC and MONU are listed in Table 2 and illustrated in Figure 9. Only the north-trending GPS displacement components are used because of the large east-trending errors inherent in the 1986 survey. The fault parallel velocities assume right-lateral displacement oriented N40°W. The VLBI measurements indicate 1.5 to 2.1 cm/yr fault-parallel (right-lateral) displacement across the San Andreas fault (BLAC-PINY) and 3.0 to 3.5 cm/yr across the Imperial Valley (BLAC-MONU). The GPS measurements indicate 1.4 cm/yr displacement across the fault and 3.2 cm/yr across the valley (the rate in Table 1 differs since it represents an average over the entire network). The BLAC-MONU velocities agree with the conventional geodetic measurements of displacement across the valley (3.4 - 4.3 cm/yr). The fault-crossing displacements (BLAC-PINY), however, are somewhat surprising since they are less than expected based on geologic evidence. The long-term geomorphological slip rate along the southern San Andreas fault over the last 10,000 - 30,000 years is estimated between 2.3 and 3.5 cm/yr [*Keller et al.*, 1982; *Weldon and Sieh*, 1985], with 2.5 cm/yr a commonly accepted average [e.g., *Sieh and Williams*, 1990]. The geologic slip rate and radiocarbon dating of Holocene offsets along the fault suggest a recurrence interval of about 300 years with the last major event in 1680 [*Sieh*, 1986]. This logic leads to the conclusion that the potential for a major earthquake along the southern San Andreas fault is high. However, the geodetic evidence reported here indicate a comparatively small strain rate during the last decade. This suggests a decreased earthquake potential for the southern San Andreas fault, assuming the geodetic measurements are indicative of at least the last few hundred years. This decreased seismic potential will be observed either as a longer recurrence interval or less slip per event. The geodetic data are supported by geologic trenching studies, which suggest a decreasing slip rate along the southern San Andreas fault during the past 1000 years [*Sieh*, 1986]. If this is true, the San Jacinto fault should play a more active role in regional tectonics. In fact, the shear strain along the fault determined from EDM observations between 1973 and 1984 is nearly the same as that for networks which lie on the San Andreas fault [*Savage et al.*, 1986]. The two fault systems may alternately assume dominant roles in absorbing plate motions, as is suggested by variable Quaternary slip rates along the San Jacinto fault [*Sharp*, 1981].

### Future analyses

The 1986, 1988, and 1989 Imperial Valley GPS observations are not sufficiently resolved to accurately map details of the strain distribution in this portion of southern California. This is due to the quality of the 1986 data, complications due to the 1987 Superstition Hills earthquake sequence, the inability to incorporate L2 phase data from several sites observed in 1989, and the short interval spanned by the measurements (1 year of nonseismic displacement). However, additional GPS data have been collected in southern California in March/April 1988 and again in February-April 1990 (Figure 10).

The 1988 measurements were made by the Riverside County (California) Flood Control District and the Riverside County Survey Department. A total of 62 stations spanning an entire cross section of southern California were occupied. Up to 8 TI-4100 GPS receivers were deployed each day over the two week survey. The daily observation period was about 4.5 hours. Although the instruments collected data every 3 seconds, only every 10th measurement was recorded during the download from receiver to floppy disk (30 second epochs). Unfortunately, the receivers were not synchronized and the recorded time-tags were randomly distributed at 30-second intervals. These data were subsequently processed with the Bernese software. The average day-to-day repeatability for the 18 line-lengths with multiple observations was 1.1 cm. Since tectonic deformation rates up to 5 cm/yr are expected in southern California, the receiver time-tag offsets should not be a serious source of error.

During 1990 (February/March), a high precision GPS network was established along a 400 km segment of the Pacific-North American plate-boundary from the Gulf of California in northern Mexico to just south of the junction of the San Andreas and San

Jacinto faults (~ 34° N) [*Reilinger et al.*, 1990]. Twenty-three receivers were used for approximately two weeks. A total of 134 stations were occupied during the campaign. Data collection at 103 sites lasted 6 to 7 hours each day, while the daily observation interval at 31 sites was 3 to 4 hours (half-sessions). The following month (April), 3 additional monuments near Upland, California, were established and surveyed by the Riverside County Flood Control District in support of university research associated with the $M_L$ 5.5 Upland earthquake of February 28, 1990. The 1990 observations are in the process of being analyzed, although obtaining geodetic coordinates for the entire survey will be time consuming due to the enormity of the data set and the uncertainty in correlating GPS measurements from different receivers.

The 1986-1990 GPS occupation summary for Riverside County, the Imperial Valley, and Baja California is listed in Table 3. A total of 183 stations have been occupied at least once (Figure 10); 85 of these have been observed at least twice. The station coverage does not include kinematic GPS measurements made on relatively short transects (few kilometer) crossing the southern San Andreas fault [K. Hudnut, personal communication, 1990]. In addition to the dense distribution within the Imperial Valley and Baja California, the established network north of the Salton Sea provides station coverage extending from the California-Arizona border to near the Pacific Ocean. This network will be used to constrain the slip distribution along the major fault systems in southern California. When combined with geologic data of fault activity, the strain estimates will better define the earthquake potential in this region. The best GPS estimate of secular strain to date is provided by the 11 displacement vectors obtain from the 1988 and 1989 surveys. Once the 1990 data are fully analyzed, the increased station density (85 stations) and longer measurement interval (at least 2 years) will yield an order of magnitude increase in strain resolution. It should be possible to assess the present-day strain accumulation rates on the major fault systems in southern California to within a few millimeters per year. The network also provides good coverage along the southern San Andreas fault, which will be used to constrain fault rupture parameters in the event of a large earthquake within the next several decades [*Larsen*, 1990].

## 6. Conclusions

GPS measurements from southern California indicate 5.9 $\pm$ 1.0 and 5.2 $\pm$ 0.9 cm/yr right-lateral southeast-trending displacement across the Imperial Valley for the intervals 1986-1988 and 1988-1989, respectively. These rates are significantly larger than those obtained from conventional geodetic surveys (3.4 - 4.3 cm/yr), suggesting the GPS observations may overestimate the true deformation. The earlier measurements contain relatively large errors, and are influenced by the 1987 Superstition Hills earthquake sequence. Regardless, secular deformation is clearly observed for both intervals, and this is attributed to the relative movement between the Pacific and North American plates. There is evidence from VLBI and GPS measurements that the strain accumulation along the southern-most San Andreas fault is smaller than the long-term geologic estimate. This indicates a lower earthquake potential for this segment of the fault than is presently assumed, and suggests that the San Jacinto system plays a more dominant role for relieving strain accumulation in this region. The measurements discussed here form part of a larger 183 station GPS network which spans an entire cross section of southern California. A total of 134 stations were observed during a recent 1990 campaign; many of these sites were previously occupied in 1986 and/or 1988. Once the 1990 GPS data are fully integrated with the previous measurements, the present-day rate of strain accumulation along the southern San Andreas, San Jacinto, and Elsinore faults will be resolvable to within a few millimeters per year.

## Acknowledgements

We thank Helen Neugebauer and Bill Strange for providing coordinate solutions from the 1986 NGS GPS survey. This research could not have taken place without the invaluable field support provided by many people. In particular, we thank John Beavan, Lewis Gilbert, Ken Hudnut, Michael Jackson, and Mike Bevis. Reviews by Hiroo Kanamori, Kerry Sieh, and William Prescott substantially improved the manuscript. This work is supported by U.S. Geological Survey contracts 14-08-0001-61679 (MIT) and 14-08-001-61354 (Caltech), and by NASA grant NAG-5-814 (MIT). Caltech Division of Geological and Planetary Sciences contribution number 4981

**References**

Anderson, J. G., and P. Bodin, Earthquake recurrence models and historical seismicity in the Mexicali-Imperial Valley, *Bull. Seismol. Soc. Am.*, *77*, 562-578, 1987.

Archuleta, R. J., A faulting model for the 1979 Imperial Valley earthquake, *J. Geophys. Res.*, *89*, 4559-4585, 1984.

Chin, M., CIGNET report, *GPS Bull.*, Global Positioning System Subcomm. of Comm. VIII, Int. Coord. of Space Tech. for Geod. and Geodyn., Natl. Geod. Surv., Rockville, Md., 1988.

Clark, T. A., D. Gordon, W. E. Himwich, C. Ma, A. Mallama, and J. W. Ryan, Determination of relative site motions in the western United States using Mark III very long baseline interferometry, *J. Geophys. Res.*, *92*, 12,741-12,750, 1987.

Davis, J. L., W. H. Prescott, J. L. Svarc, and K. J. Wendt, Assessment of global positioning system measurements for studies of crustal deformation, *J. Geophys. Res.*, *94*, 13,635-13,650, 1989.

DeMets, C., R. G. Gordon, S. Stein, and D. F. Argus, A revised estimate of Pacific-North America motion and implications for western North America plate boundary zone tectonics, *Geophys. Res. Letts.*, *14*, 911-914, 1987.

DeMets, C., R. G. Gordon, D. F. Argus, and S. Stein, Current plate motions, *Geophys. J. Inter.*, *101*, 425-478, 1990.

Dong, D., and Y. Bock, Global Positioning System network analysis with phase ambiguity resolution applied to crustal deformation studies in California, *J. Geophys. Res.*, *94*, 3949-3966, 1989.

Drew, A. R., and R. A. Snay, DYNAP: software for estimating crustal deformation from geodetic data, *Tectonophysics, 162*, 331-343, 1989.

Elders, W. A., R. W. Rex, T. Meidav, P. T. Robinson, and S. Biehler, Crustal spreading in southern California, *Science, 178*, 15-24, 1972.

Fuis, G. S., W. D. Mooney, J. H. Healey, G. A. McMechan, and W. J. Lutter, Crustal structure of the Imperial Valley region, *U.S. Geol. Surv. Prof. Pap., 1254*, 25-50, 1982.

Hartzell, S. H., and T. H. Heaton, Inversion of strong ground motion and teleseismic waveform data for the fault rupture history of the 1979 Imperial Valley, California, earthquake, *Bull. Seis. Soc. Am., 73*, 1553-1583, 1983.

Ingle, J. C., Paleobathymetric history of Neogene marine sediments, northern Gulf of California, *in* Geology of Peninsular California, Pacific Sections AAPG, SEPM, and SEG, 121-138, 1974.

Jackson, M., R. Reilinger, M. Bevis, B. Perin, C. Rocken, B. Stephens, and J. Stowell, Impact of ionospheric effects on GPS campaigns in southern California and the South Pacific, *EOS Trans., 70*, p. 1049, 1989.

Johnson, C. E., and D. P. Hill, Seismicity of the Imperial Valley, *U.S. Geol. Surv. Prof. Pap., 1254*, 14-24, 1982.

Keller, E. A., M. S. Bonkowski, R. J. Korsch, and R. J. Shiemon, Tectonic geomorphology of the San Andreas fault zone in the southern Indio Hills, Coachella Valley, California, *Geol. Soc. Am. Bull., 93*, 46-56, 1982.

King, R. W., E. G. Masters, C. Rizos, A. Stolz, and J. Collins, *Surveying with GPS, Monograph 9*, School of Surveying, The University of New South Wales, Kensington, Australia, 1985.

Kroger, P. M., G. A. Lyzenga, K. S. Wallace, and J. M. Davidson, Tectonic motion in the western United States inferred from very long baseline interferometry measurements, 1980-1986, *J. Geophys. Res.*, *92*, 14,151-14163, 1987.

Larsen, S. C., Inverting GPS displacement vectors for seismic slip distribution: Implications for network geometry along the southern San Andreas fault, paper presented at NSF/USGS joint workshop: crustal deformation measurement and earthquake mechanics, Morro Bay, California, 1990.

Larsen, S. C., R. E. Reilinger, H. Neugebauer, W. Strange, GPS measurements of deformation associated with the 1987 Superstition Hills earthquake, Imperial Valley, California: Evidence for conjugate faulting, *J. Geophys. Res.*, submitted, 1991a.

Larsen, S. C., D. C. Agnew, B. H. Hager, Strain accumulation in the Santa Barbara channel: 1970-1988, in preparation, 1991b.

Larson, P. A., H. W. Menard, and S. M. Smith, Gulf of California: A result of ocean-floor spreading and transform faulting, *Science*, *161*, 781-784, 1968.

Lomnitz, C., F. Mooser, C. R. Allen, J. N. Brune, and W. Thatcher, Seismicity and tectonics of northern Gulf of California region, Mexico: Preliminary results, *Geofis. Int.*, *10*, 34-48, 1970.

Ma, C., J. W. Ryan, D. Caprette, Crustal dynamics project data analysis -- 1988, VLBI geodetic results 1979-1988, *NASA Technical Memorandum*, *100723*, 1989.

Magistrale, H., L. Jones, and H. Kanamori, The Superstition Hills, California, earthquakes of 24 November, 1987, *Bull. Seismol. Soc. Am.*, *79*, 239-251, 1989.

Mansinha, L., and D. E. Smylie, The displacement fields of inclined faults, *Bull. Seismol. Soc. Am.*, *61*, 1433-1440, 1971.

Moore, D. G., and E. C. Buffington, Transform faulting and growth of the Gulf of California since late Pliocene, *Science, 161*, 1238-1241, 1968.

Prescott, W. H., J. C. Savage, and M. Lisowski, Crustal strain, in National Earthquake Hazards Reduction Program, Summaries of Technical Reports, *U.S. Geol. Surv. Open-File Rep., 87-374*, 272-280, 1987a.

Prescott, W. H., M. Lisowski, and J. C. Savage, Velocity field along the San Andreas fault in southern California, *EOS Trans., 68*, p. 1506, 1987b.

Reilinger, R., Coseismic and postseismic vertical movements associated with the 1940 M7.1 Imperial Valley, California, earthquake, *J. Geophys. Res., 89*, 4531-4537, 1984.

Reilinger, R. E., and S. C. Larsen, Vertical crustal deformation associated with the 1979 M = 6.6 Imperial Valley, California earthquake: Implications for fault behavior, *J. Geophys. Res., 91*, 14,044-14,056, 1986.

Reilinger, R., J. Beavan, L. Gilbert, S. Larsen, K. Hudnut, C. Aiken, D. Ziegler, B. Strange, M. F. de la Fuente, J. G. Garcia, J. Stowell, W. Young, G. Doyle, and G. Stayner, 1990 Salton Trough-Riverside County GPS Network, *EOS Trans. abst., 71*, p. 447, 1990.

Sauber, J., Geodetic measurement of deformation in California, Ph.D. Thesis, Massachusetts Institute of Technology, 1989.

Savage, J. C., W. H. Prescott, M. Lisowski, and N. King, Deformation across the Salton Trough, California, 1973-1977, *J. Geophys. Res., 84*, 3069-3079, 1979.

Savage, J. C., W. H. Prescott, M. Lisowski, and N. E. King, Strain accumulation in Southern California, 1973-1980, *J. Geophys. Res., 86*, 6991-7001, 1981.

Savage, J. C., W. H. Prescott, and G. Gu, Strain accumulation in southern California, 1973-1984, *J. Geophys. Res.*, *91*, 7455-7473, 1986.

Sharp, R. V., Variable rates of late Quaternary strike slip on the San Jacinto fault zone, southern California, *J. Geophys. Res.*, *86*, 1754-1762, 1981.

Sharp, R. V., Comparison of 1979 surface faulting with earlier displacements in the Imperial Valley, *U.S. Geol. Surv. Prof. Pap.*, *1254*, 213-221, 1982.

Sieh, K. E., Slip rate across the San Andreas fault and prehistoric earthquakes at Indio, California, *Eos Trans. abst.*, *67*, p. 1200, 1986.

Sieh, K. E., and P. L. Williams, Behavior of the southernmost San Andreas fault during the past 300 years, *J. Geophys. Res.*, *95*, 6629-6645, 1990.

Snay, R. A., and A. R. Drew, Supplementing geodetic data with prior information for crustal deformation in the Imperial Valley, California, Technical Report Series, University of Stuttgart, 30 p., 1988.

Sykes, L. R., and S. P. Nishenko, Probabilities of occurrence of large plate rupturing earthquakes for the San Andreas, San Jacinto, and Imperial faults, California, 1983-2003, *J. Geophys. Res.*, *89*, 5905-5927, 1984.

Thatcher, W., Horizontal crustal deformation from historic geodetic measurements in southern California, *J. Geophys. Res.*, *84*, 2351-2370, 1979.

Trifunac, M. D., and J. N. Brune, Complexity of energy release during the Imperial Valley, California, earthquake of 1940, *Bull. Seismol. Soc. Am.*, *60*, 137-160, 1970.

Weldon, R. J., and K. E. Sieh, Holocene rate of slip and tentative recurrence interval for large earthquakes on the San Andreas fault, Cajon Pass, southern California, *Geol. Soc. Am. Bull.*, *96*, 793-812, 1985.

U. S. G. S., The Imperial Valley, California, earthquake of October 15, 1979, *U.S. Geol. Surv. Prof. Pap.*, *1254*, 451 p., 1982.

Table 1. Displacement Rates

| Method | Region | Interval | Rate (cm/yr) | Reference |
|---|---|---|---|---|
| GPS | Imperial Valley | 1986-1988 | 5.9 | This Study |
| | | 1988-1989 | 5.2 | |
| Triangulation | Imperial Valley | 1941-1986 | 4.3 | *Snay and Drew* [1988] |
| | | 1941-1954 | 6.1 | |
| | | 1954-1967 | 2.1 | |
| | | 1967-1986 | 4.5 | |
| Trilateration | Imperial Valley | 1972-1987 | 3.4 | *Prescott et al.* [1987b] |
| Plate Model | Plate boundary | $\sim$ 3 m.y. | 4.7 | *DeMets et al.* [1990] |
| VLBI | Continental | 1979-1987 | 4.8-5.1 | *Clark et al.* [1987] |
| | | | | *Kroger et al.* [1987] |

Table 2. Displacement Rates Across San Andreas Fault

| Baseline | Method | Interval | North (cm/yr) | East (cm/yr) | Fault Parallel (cm/yr) |
|---|---|---|---|---|---|
| BLAC-PINY | VLBI[1] | 1982-1987 | 1.8 | -1.1 | 2.1 |
| | VLBI[2] | 1979-1988 | 1.5 | -1.0 | 1.8 |
| | VLBI[3] | 1982-1988 | 1.2 | -0.9 | 1.5 |
| | GPS | 1986-1988 | 1.1 | | 1.4 |
| BLAC-MONU | VLBI[1] | 1982-1987 | 2.3 | -2.7 | 3.2 |
| | VLBI[2] | 1979-1988 | 2.5 | -2.5 | 3.5 |
| | VLBI[3] | 1982-1988 | 2.4 | -1.8 | 3.0 |
| | GPS | 1986-1989 | 2.5 | | 3.2 |

[1] *Clark et al.* [1987]
[2] *Ma* [1988]
[3] *Sauber* [1989]

Table 3. GPS Campaign Summary

| Year | Stations | Region | Organization |
|---|---|---|---|
| 1986 | 42 | Imperial Valley | NGS |
| 1988 | 15 | Imperial Valley | UNAVCO |
| 1988 | 62 | Riverside County | RCFC/RCSD |
| 1988 | 21 | Imperial Valley | NGS |
| 1989 | 28 | Imperial Valley | UNAVCO |
| 1990 | 134 | Imperial Valley/Riverside County | UNAVCO/RCFC/RCSD/NGS |

NGS - National Geodetic Survey
UNAVCO - University Navstar Consortium
RCFC - Riverside County Flood Control
RCSD - Riverside County Survey District

## Figure Captions

**Figure 1:** Major faults and seismicity from 1932 to 1990 (Caltech Catalog) in the Imperial Valley. Large earthquakes are shown as stars. The Brawley Seismic Zone is the region of anomalously high activity between the Imperial and San Andreas faults. Major earthquakes include the 1940 and 1979 events along the Imperial fault, the 1954 and 1968 events along the San Jacinto fault, and the 1987 Superstition Hills earthquake sequence along the Superstition Hills and Elmore Ranch faults.

**Figure 2:** GPS stations surveyed in 1986 and 1988. The 1986 campaign was conducted by the National Geodetic Survey and included 42 stations in and near the Imperial Valley. The 1988 observations consisted of two campaigns, the first by university groups in February/March and the second by the National Geodetic Survey in March/April. A total of 32 stations were occupied in 1988, of which 29 were repeat measurements from 1986. Stations mentioned in text are indicated.

**Figure 3:** Imperial Valley GPS stations surveyed in 1989. TI-4100 GPS receivers (triangles) were used at most sites. Trimble 4000sd receivers (open circles) were also used. Thirty sites were occupied; 10 for the first time. Due to very poor ionospheric conditions, data collected with the Trimble 4000SD receivers are not discussed here.

**Figure 4:** GPS station displacements for the interval 1986-1988 (1.8 years). All measurements are made relative to station OCTI. Errors are determined by multiplying the formal uncertainties from the GPS solution by a variance factor so that the average baseline error scales as 1 ppm. The east-west uncertainties are about 4 times larger then the north-south. Seismically induced displacements from the 1987 Superstition Hills earthquake sequence are most apparent at stations KANE and L589. The large non-seismic displacements are assumed to represent relative motion between the Pacific and North American plates, which is concentrated across

the valley.

**Figure 5:** GPS station displacements for the interval 1988-1989 (1.0 years). All measurements are made relative to station OCTI. Errors are determined by multiplying the formal uncertainties from the GPS solution by a variance factor so that the average baseline error scales as 0.5 ppm. Stations to the northeast moved about 5 cm southwest relative to stations on the other side of the valley.

**Figure 6:** The north-south and east-west displacement components for the 1986-1988 interval. All distances are relative to OCTI on a cross section trending N50°E, perpendicular to the plate motion (see Figure 8). The effect of the 1987 Superstition Hills earthquake sequence is removed. Open circles indicate stations where the seismic correction is greater than 4 cm. The north-south offset between stations on opposite sides of the valley is 8.1 cm. The large scatter for the east-west components are presumably due to errors in the 1986 survey. The average uncertainty for each displacement component is shown.

**Figure 7:** The north-south and east-west displacement components for the 1988-1989 interval. All distances are relative to OCTI on a cross section trending N50°E, perpendicular to the plate motion direction. The data are best-fit by 5.2 cm/yr displacement across the valley (solid line), although a rate of 3.4 cm/yr fit the data nearly as well (dashed line). The average uncertainty for each displacement component is shown.

**Figure 8:** Shear plane (10 km depth) used to model the 1988-1989 displacements (shaded band); cross section used in Figures 6 and 7; and stations surveyed at least twice between 1986 and 1989. Considerable strain is observed across the GPS network, which is attributed to plate-boundary deformation between the North American and Pacific plates.

**Figure 9:** VLBI (solid arrows) and GPS (dashed arrows) velocities at stations PINY and MONU relative to station BLAC (Table 2). The GPS vectors contain large uncertainty in the east-west direction. The fault-parallel geodetic velocities across the San Andreas fault are less than geologic estimates.

**Figure 10:** GPS stations occupied from 1986 to 1990 in Riverside County, the Imperial Valley, and northern Baja California. Triangles inside circles indicate stations with multiple occupations. The network is composed of 183 stations, of which 85 have repeated observations.

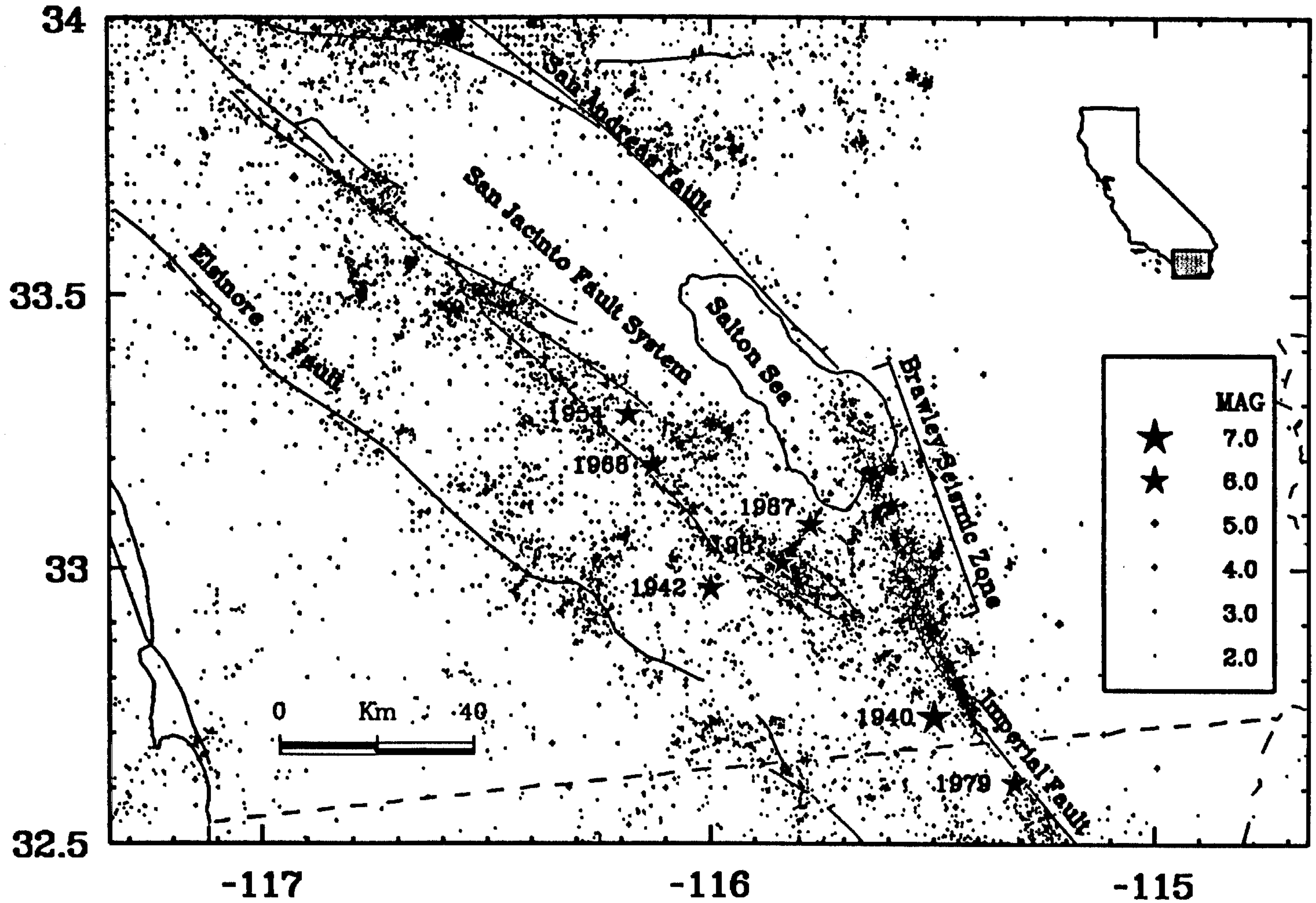
34
33.5
33
32.5
-117
-116
-115
San Andreas Fault
San Jacinto Fault System
Elsinore Fault
Salton Sea
Brawley Seismic Zone
Imperial Fault
1954
1968
1987
1987
1942
1940
1979
0
Km
40
MAG
7.0
6.0
5.0
4.0
3.0
2.0

Figure 1

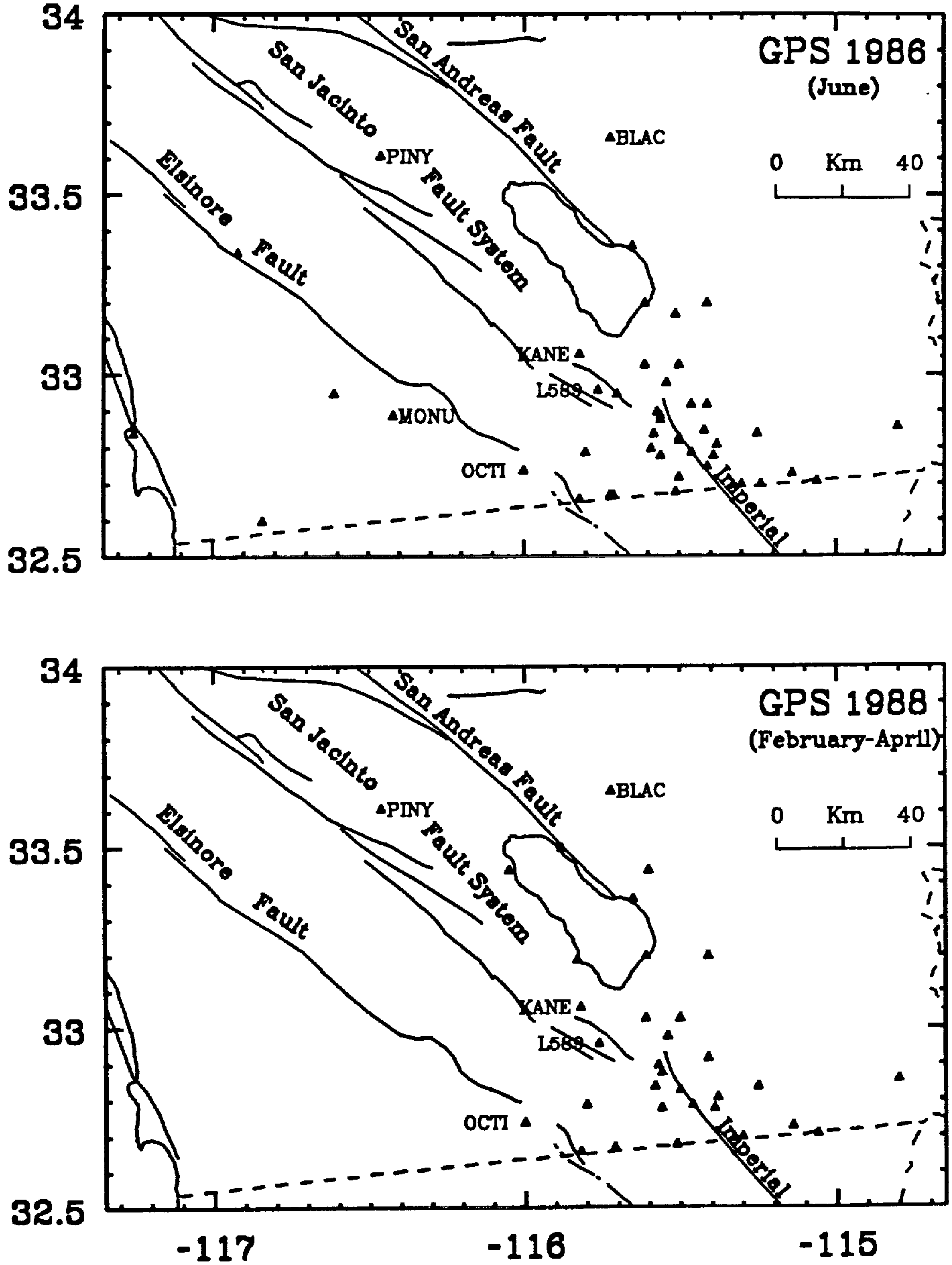
GPS 1986
(June)
0 Km 40
San Andreas Fault
San Jacinto
Fault System
Elsinore
Fault
Imperial
BLAC
PINY
KANE
L589
MONU
OCTI
34
33.5
33
32.5
GPS 1988
(February-April)
0 Km 40
San Andreas Fault
San Jacinto
Fault System
Elsinore
Fault
Imperial
BLAC
PINY
KANE
L589
OCTI
34
33.5
33
32.5
-117
-116
-115

Figure 2

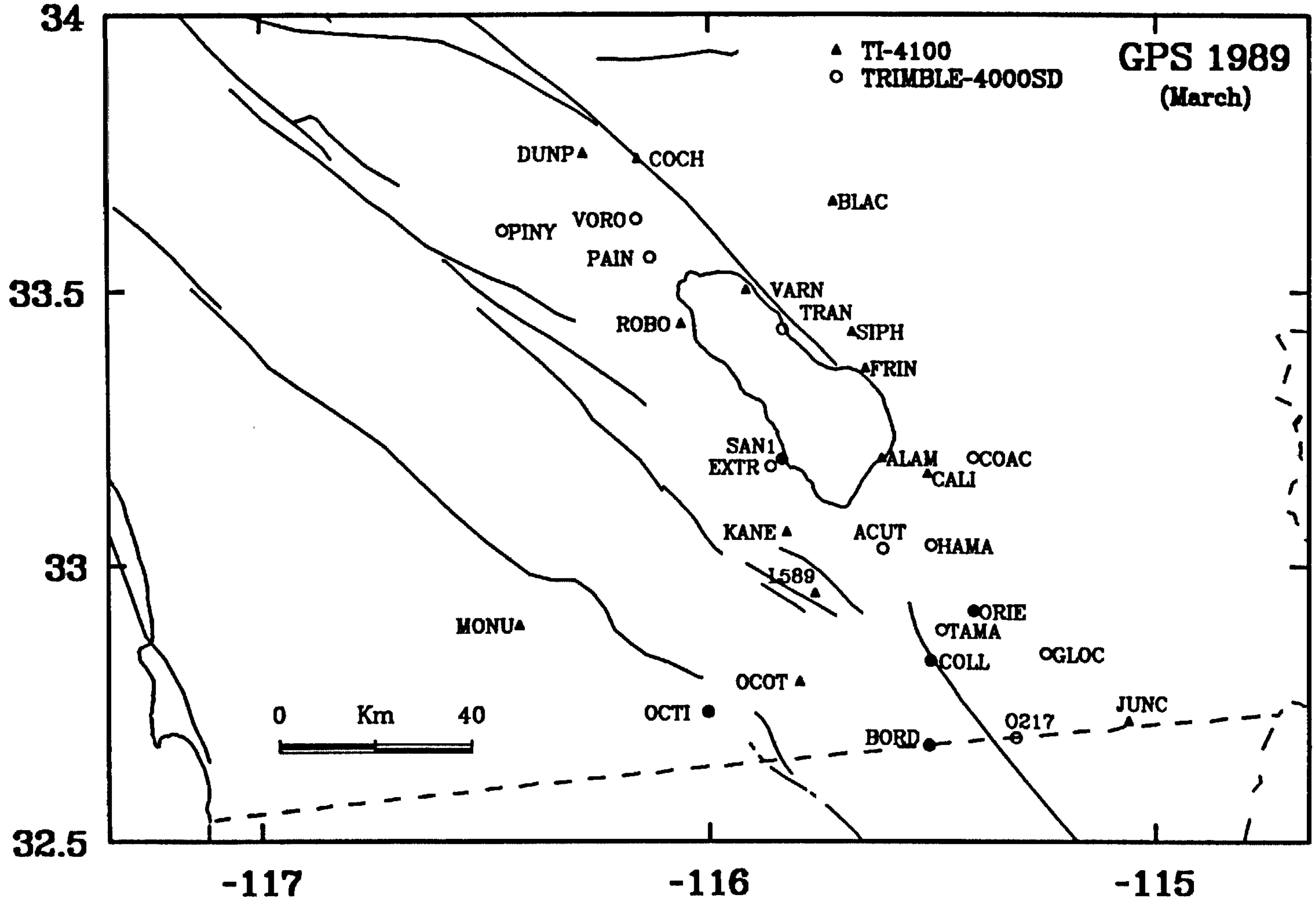
GPS 1989
(March)
TI-4100
TRIMBLE-4000SD
DUNP
COCH
BLAC
PINY
VORO
PAIN
VARN
TRAN
SIPH
ROBO
FRIN
SAN1
EXTR
ALAM
COAC
CALI
KANE
ACUT
HAMA
1589
ORIE
TAMA
MONU
COLL
GLOC
OCOT
JUNC
OCTI
0217
BORD
0
Km
40
34
33.5
33
32.5
-117
-116
-115

Figure 3

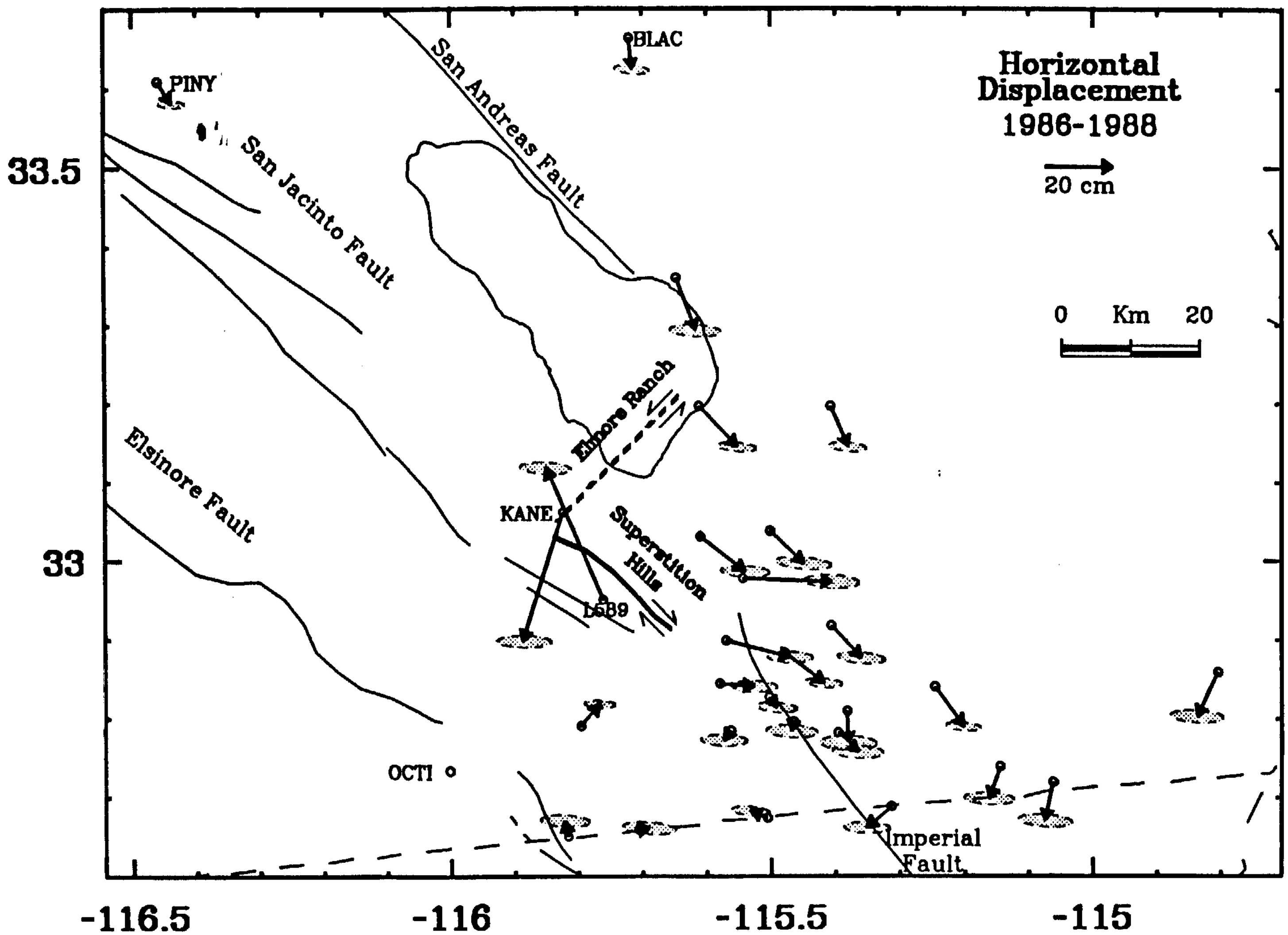
Horizontal
Displacement
1986-1988
20 cm
0 Km 20
PINY
BLAC
San Andreas Fault
San Jacinto Fault
Elsinore Fault
Elmore Ranch
Superstition
Hills
KANE
L589
OCTI
Imperial
Fault
33.5
33
-116.5
-116
-115.5
-115

Figure 4

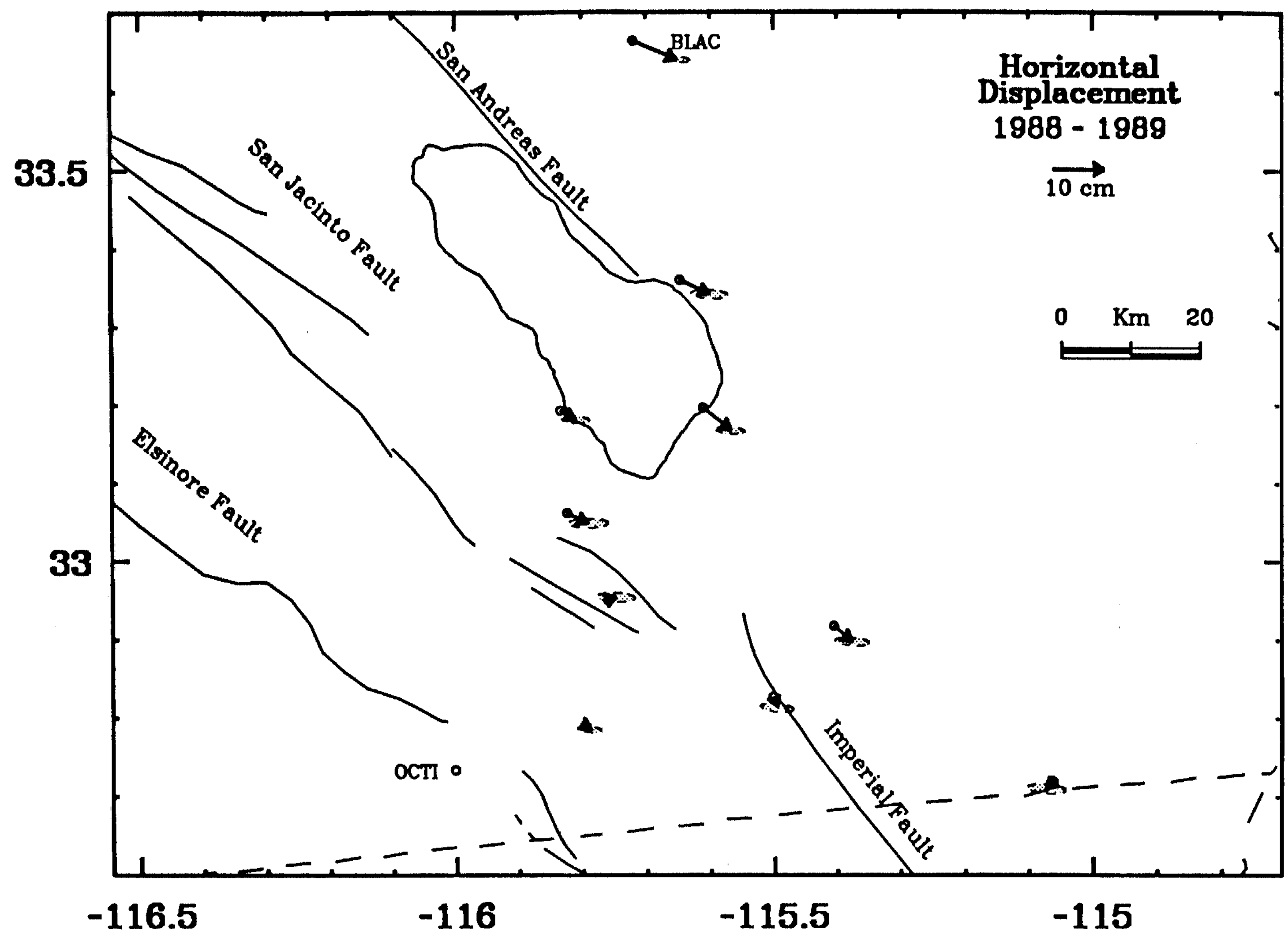

Horizontal
Displacement
1988 - 1989
10 cm
0 Km 20
BLAC
San Andreas Fault
San Jacinto Fault
Elsinore Fault
Imperial Fault
OCTI
33.5
33
-116.5
-116
-115.5
-115


Figure 5

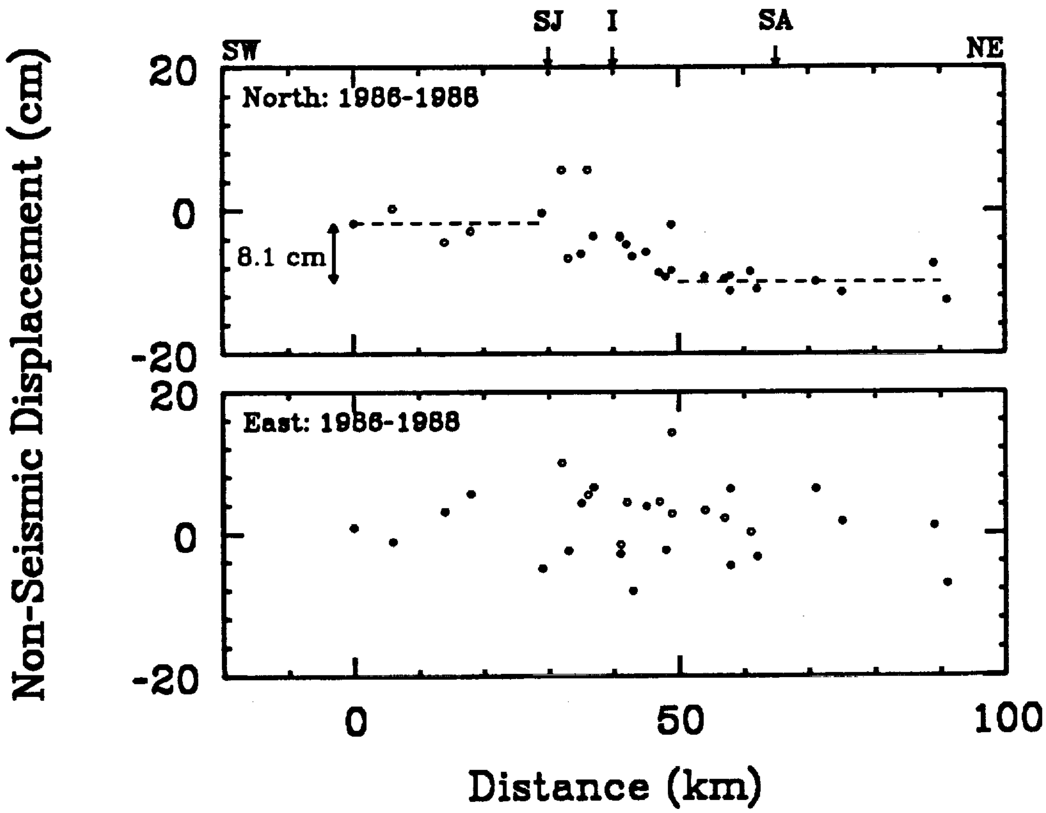
SJ
I
SA
SW
NE
North: 1986-1988
8.1 cm
East: 1986-1988
20
0
-20
0
50
100
Non-Seismic Displacement (cm)
Distance (km)

Figure 6

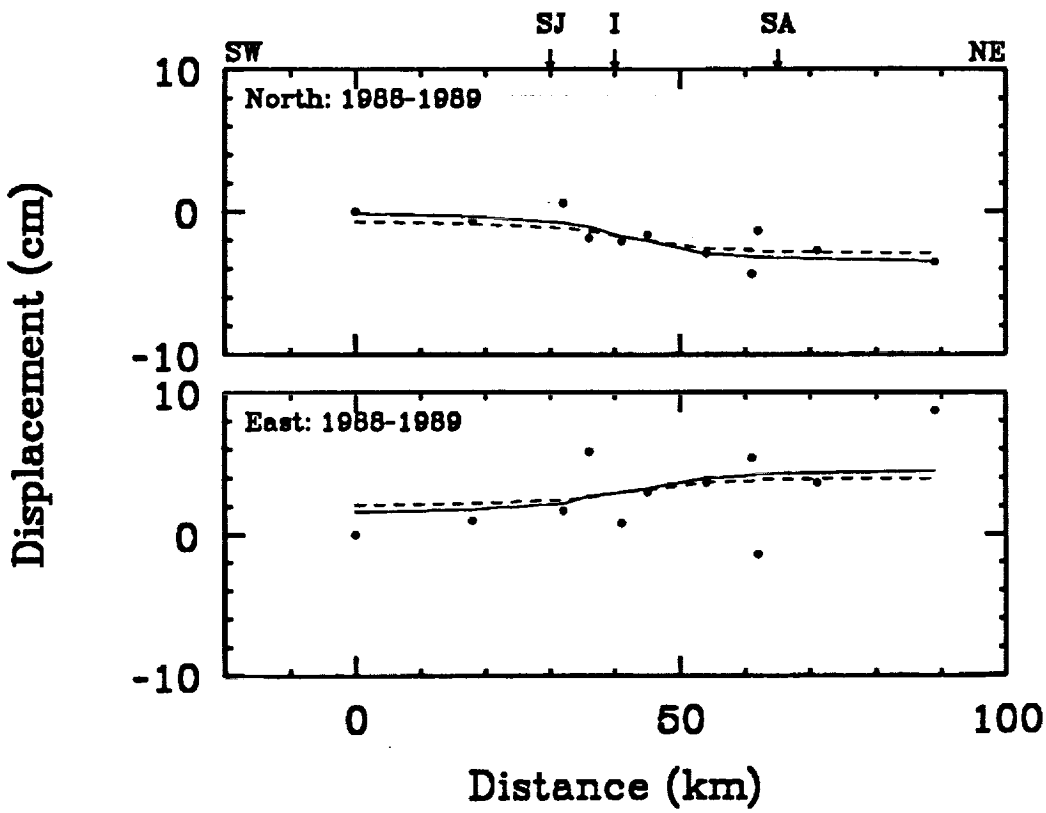

SJ
I
SA
SW
NE
10
North: 1988-1989
0
-10
10
East: 1988-1989
0
-10
0
50
100
Displacement (cm)
Distance (km)


Figure 7

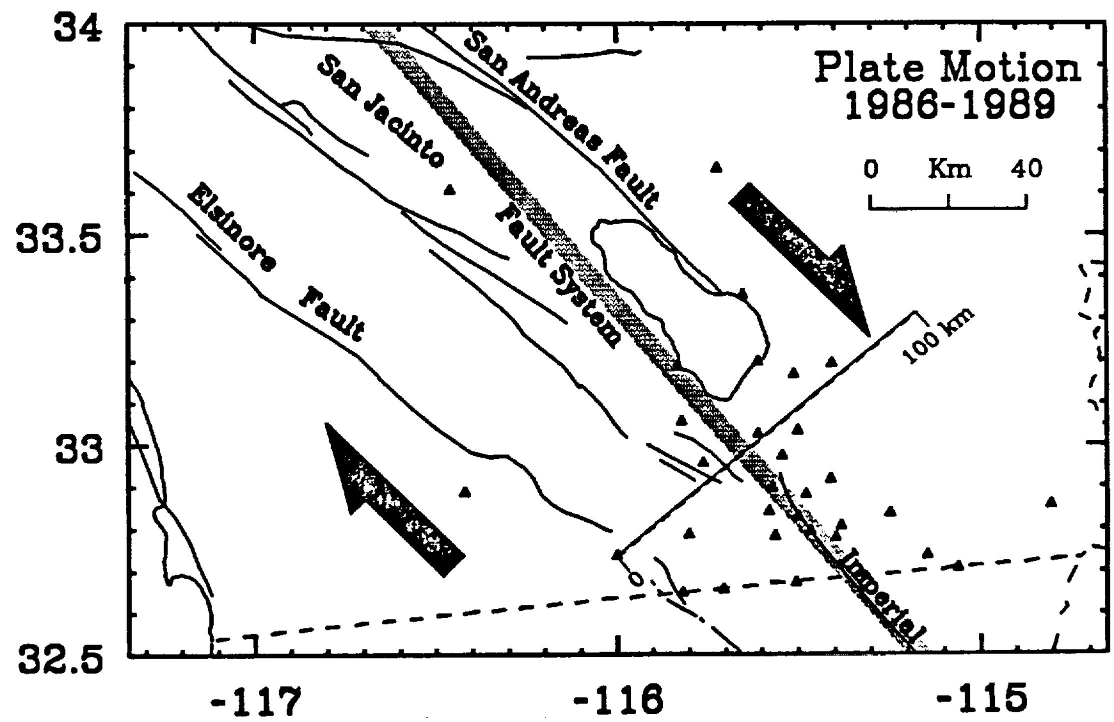

Plate Motion
1986-1989
0 Km 40
San Andreas Fault
San Jacinto
Fault System
Elsinore Fault
Imperial
100 km
34
33.5
33
32.5
-117
-116
-115


Figure 8

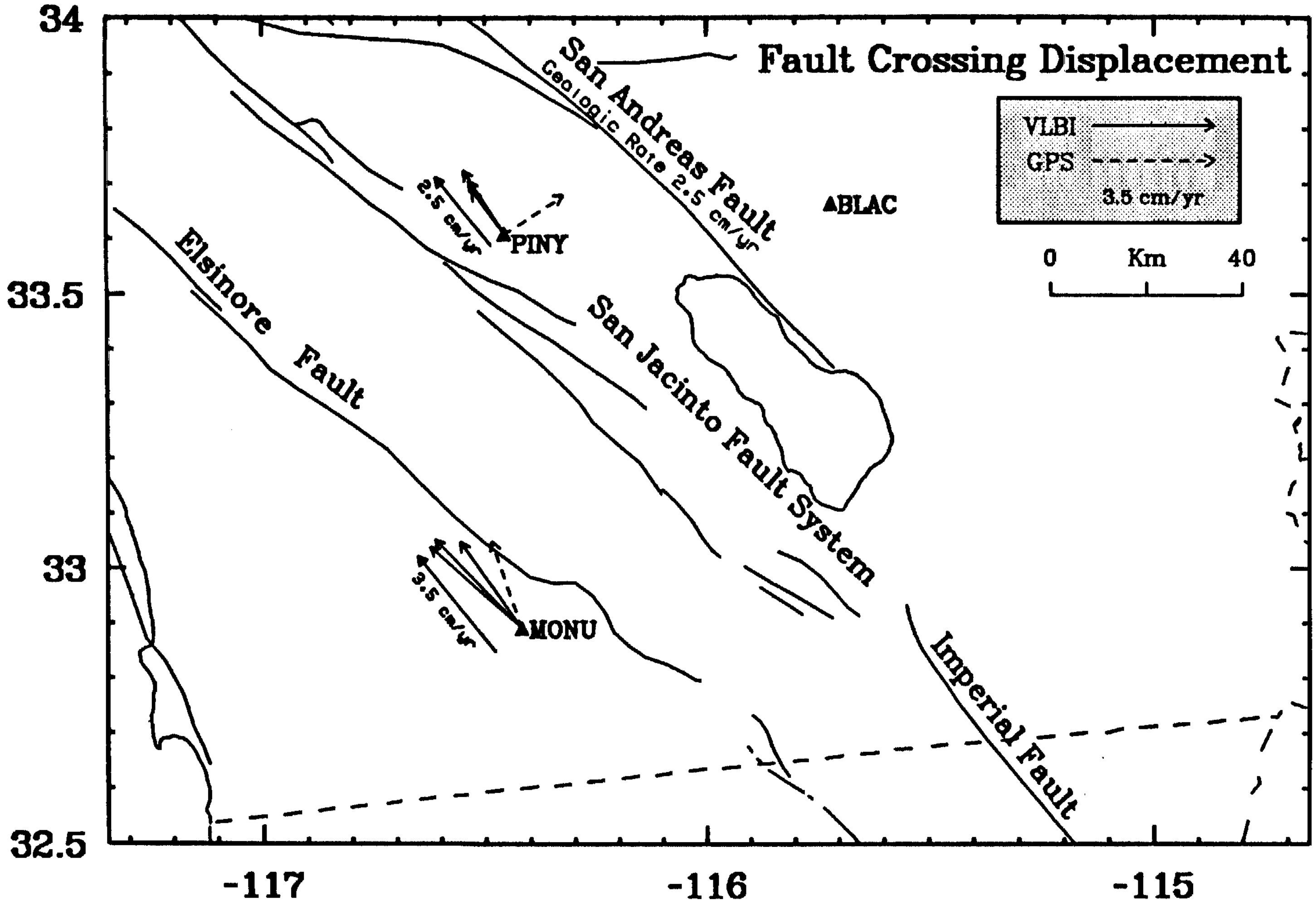
Fault Crossing Displacement
VLBI
GPS
3.5 cm/yr
0
Km
40
San Andreas Fault
Geologic Rate 2.5 cm/yr
BLAC
PINY
2.5 cm/yr
San Jacinto Fault System
Elsinore Fault
MONU
3.5 cm/yr
Imperial Fault
34
33.5
33
32.5
-117
-116
-115

Figure 9

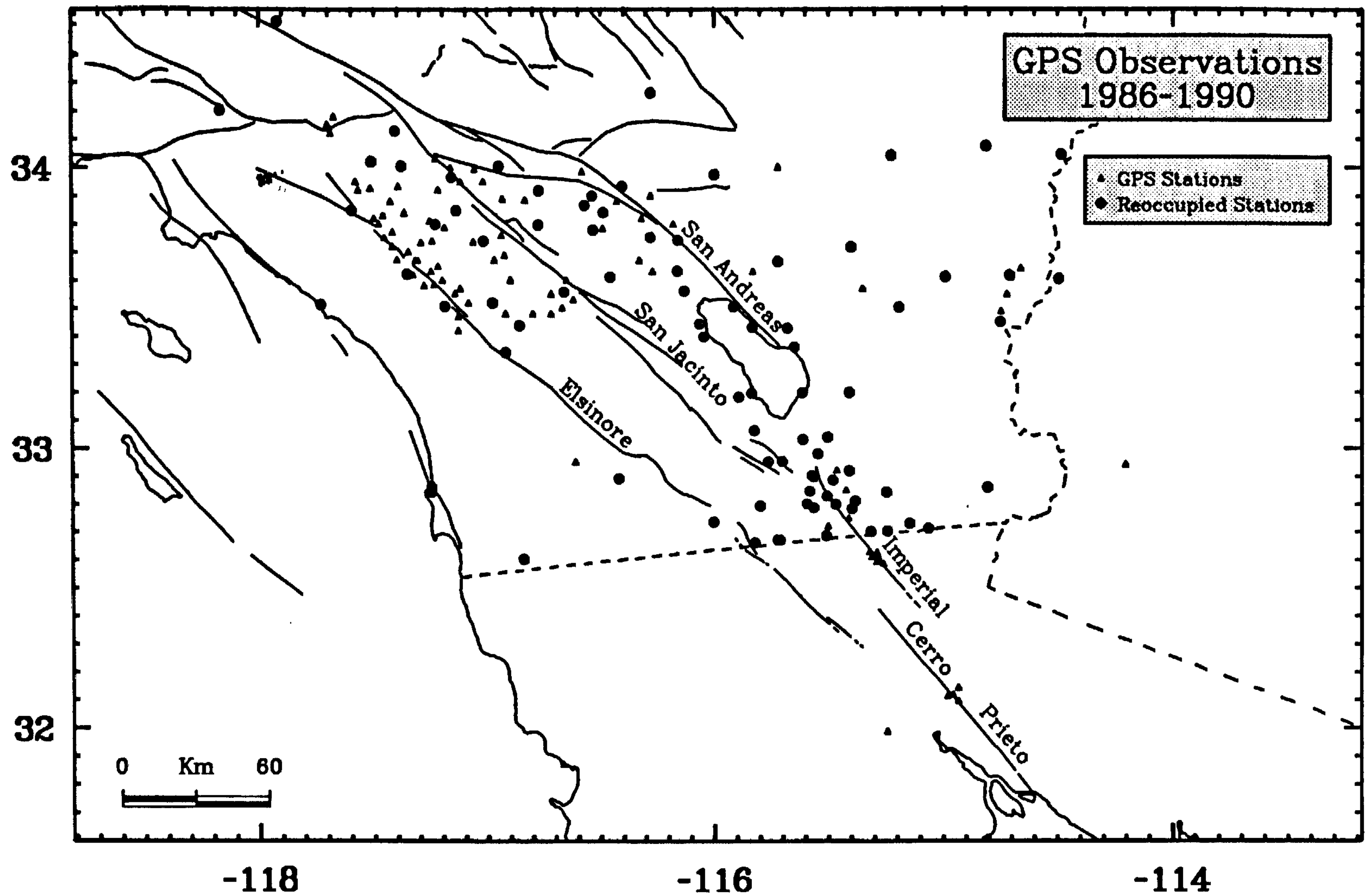
GPS Observations
1986-1990
GPS Stations
Reoccupied Stations
San Andreas
San Jacinto
Elsinore
Imperial
Cerro
Prieto
0
Km
60
34
33
32
-118
-116
-114

Figure 10